Electronic Supplementary Information (ESI)

Hierarchical NiO Mesocrystals with Tuneable High-Energy Facets for Pseudocapacitive Charge Storage

Mingtao Zheng,[a,b,c,] Hanwu Dong,[a,b] Yong Xiao,[b] Hang Hu,[a] Chenglong He,[a] Yeru Liang,[a] Bingfu Lei,[a,b] Luyi Sun,[c,]* and Yingliang Liu[a,b,]**

[a] Department of Materials Science and Engineering, College of Materials and Energy, South China Agricultural University, Guangzhou 510642, China

[b] Guangdong Provincial Engineering Technology Research Center for Optical Agriculture, Guangzhou 510642, China

[c] Department of Chemical & Biomolecular Engineering and Polymer Program, Institute of Materials Science, University of Connecticut, Storrs 06269, USA

Experimental

Materials. Nickel acetate tetrahydrate [$Ni(COOCH_3)_2 \cdot 4H_2O$, $Ni(Ac)_2$], carbon black, and polytetrafluoroethylene (PTFE) were purchased from Sigma-Aldrich. Absolute ethanol and potassium hydrate (KOH) were purchased from Guangzhou Chemical Reagent Factory (China). All the chemical reagents were analytically pure and used as received without further purification.

Synthesis of Hierarchically Structured NOMs. The cuboctahedral NOMs were synthesized by a simple hydrothermal method without involving any expensive organic additives and post-treatment process. In a typical procedure, 4.0 g of $Ni(Ac)_2$ was magnetically stirred in 40 mL of ethanol solution with various volume ratio ($V_{ethanol}/V_{H2O}$) for 30 min to form a homogeneous solution, which was then sealed into a steel-stainless autoclave with 50 mL of capacity. Subsequently, the autoclave was placed in an electronic furnace, and then heated to 400 ºC at a heating rate of 10 ºC min^{-1} and maintained at this temperature for 12 h. After cooling down to room temperature naturally, the greyish-green powders were collected and washed with de-ionized water and ethanol for several times, and then dried at 60 ºC overnight. The as-prepared samples were denoted as "NOM-x", where x represents the volume of ethanol (mL).

Characterization of NiO Mesostructures. The samples were characterized by X-ray diffraction (XRD, MSAL-XD2, Cu Kα, λ=0.15406 nm). The morphology of the samples was characterized by field emission scanning electron microscopy (FESEM, Zeiss Ultra 55), transmission electron microscopy (TEM), and high resolution TEM (HRTEM, JEM-2100F). The porosity of the as-prepared NOMs was determined from N_2 adsorption/desorption isotherms measured at 77 K using an automatic volumetric sorption analyzer (ASAP 2020 HD88, Micromeritics Instrument Corp.).

Electrochemical Measurements. The working electrode was prepared by pressing a mixture of active materials, carbon black, and 5% PTFE (75:15:10 wt %) into a current collector of a foam nickel electrode under 35 MPa. All electrochemical measurements were performed on an IviumStat electrochemical workstation at room temperature. The experiments were carried out in a standard three electrodes cell, a nickel foil as counter electrode, a saturated calomel electrode (SCE) as reference electrode, and the above mentioned electrode as working electrode. The working electrode was measured by cyclic voltammetry (CV), galvanostatic charge/discharge, and electrochemical impedance spectroscopy (EIS) in 2.0 M KOH aqueous solution.

Specific capacitance was calculated from the CV curves by using **Eq. 1**:

$$C = \frac{Q}{mV} = \frac{\int I\mathrm{d}t}{m\Delta V} \quad (1)$$

where I is the oxidation or reduction current, dt is the time differential, m indicates the mass of the active electrode material, and ΔV indicates the voltage range of one sweep segment. Specific capacitance could also be calculated from the galvanostatic charge and discharge curves by using **Eq. 2**:

$$C = \frac{I \times \Delta t}{m \times \Delta V} \quad (2)$$

where I is the charge or discharge current, Δt is the discharge time, m indicates the mass of the active material, and ΔV represents the voltage change after a full charge or discharge. The hybrid supercapacitor was assembled by using NOM-20 and the three-dimensional nitrogen-doped graphene (3DNG), which was prepared as previously reported,[S1] as the positive and negative electrodes in 2.0 M KOH with one piece of cellulose paper as the separator. The mass ratio between the positive and negative electrodes was determined based on **Eq. 3**:[S2]

$$\frac{m_+}{m_-} = \frac{C_- \times V_-}{C_+ \times V_+} \quad (3)$$

where m, C, and V correspond the mass of the active material, capacitance, and potential window of the electrode, respectively. The subscripts "+" and "-" represent the positive and negative electrode, respectively. According to the specific capacitances (334 F g^{-1} for 3DNG and 1039 F g^{-1} for NOM-20) and the potential windows for the 3DNG and NOM-20 electrodes, the optimal mass ratio can be calculated to be $m_+/m_- = 0.64$ for the hybrid supercapacitor. The energy density and power density were calculated from **Eqs. 4** and **5**:

$$E = \frac{0.5 \times CV^2}{3.6} \quad (4)$$

$$P = \frac{3600 \times E}{t} \quad (5)$$

where E (Wh kg^{-1}) and P (W kg^{-1}) are the energy density and power density, respectively. The definitions of C, V, and t are the same as those in **Eq. 2**, in which the specific capacitance (C) of the hybrid supercapacitor was calculated based on the total mass of active material (including NOM-20 and 3DNG).

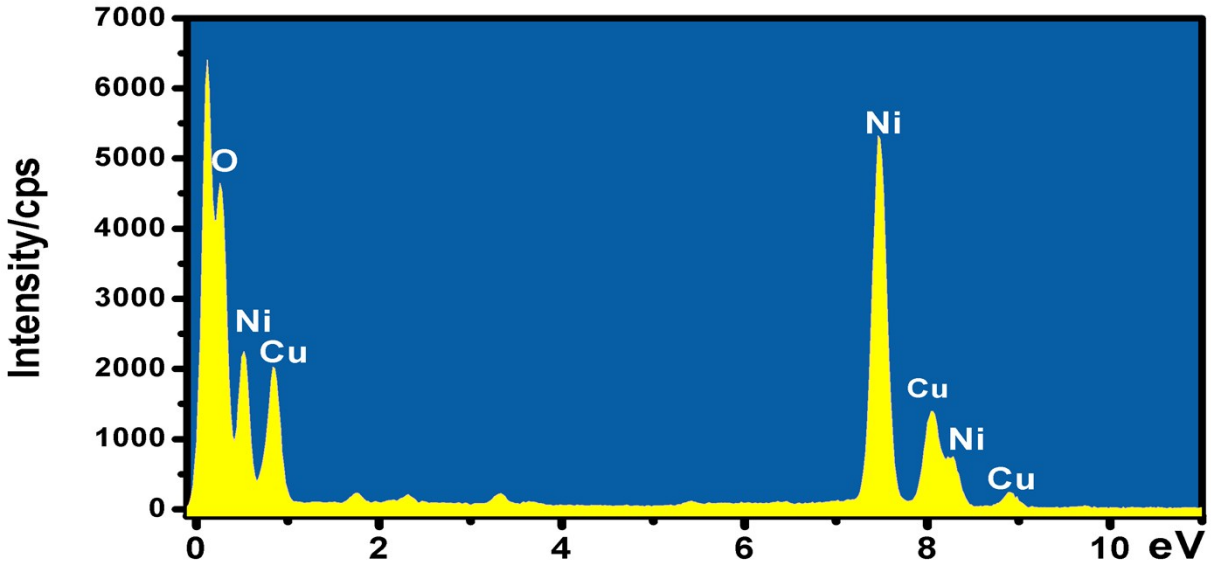

Fig. S1. EDX spectrum of the as-prepared NOM-20 at 400 ˚C for 12 h.

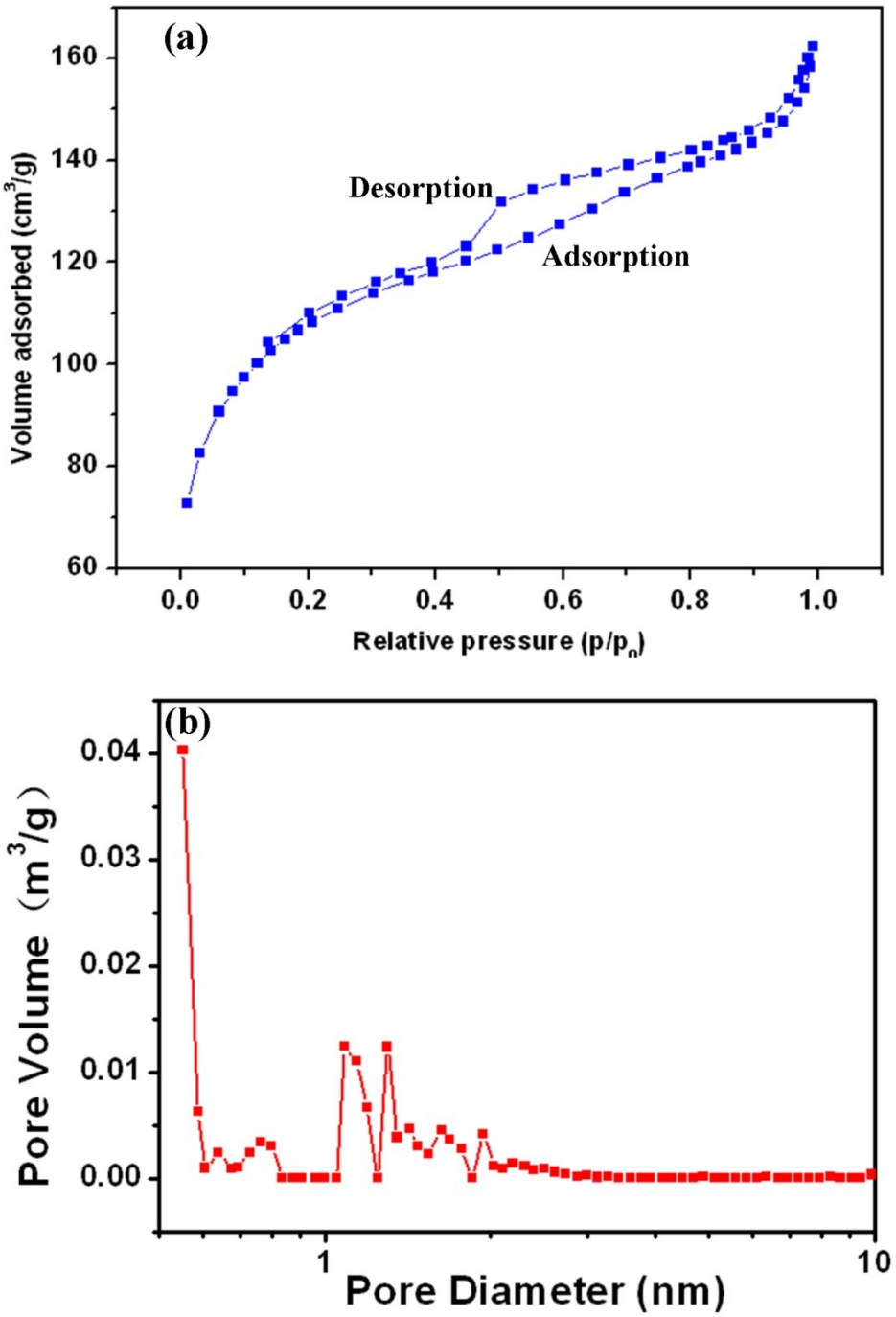

Fig. S2. (a) N_2 adsorption-desorption isotherms and (b) pore diameter curve of the as-prepared NOM-20.

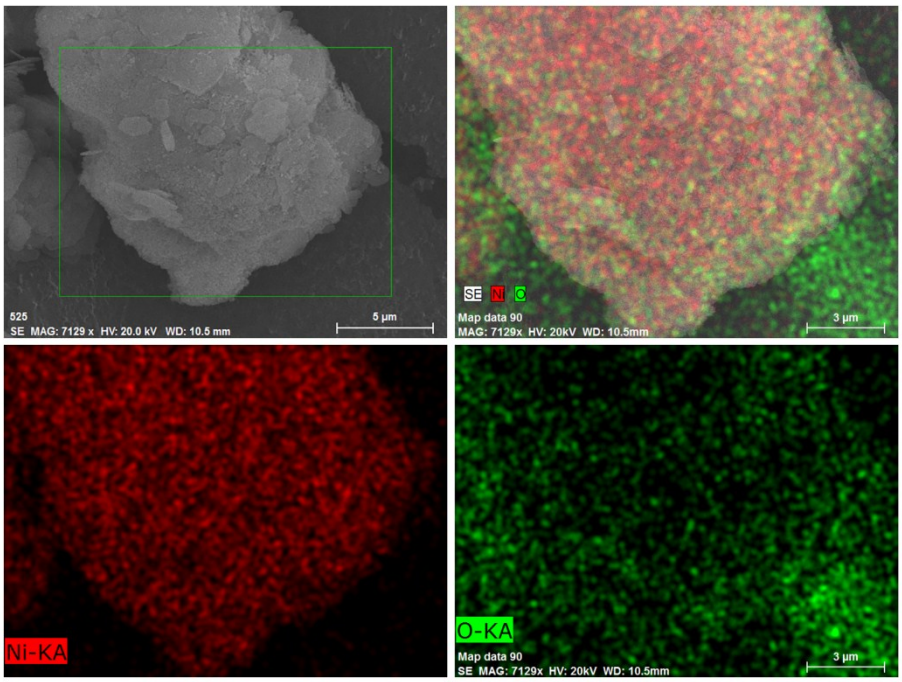

Fig. S3. Element mapping image of the as-obtained NiO aggregates.

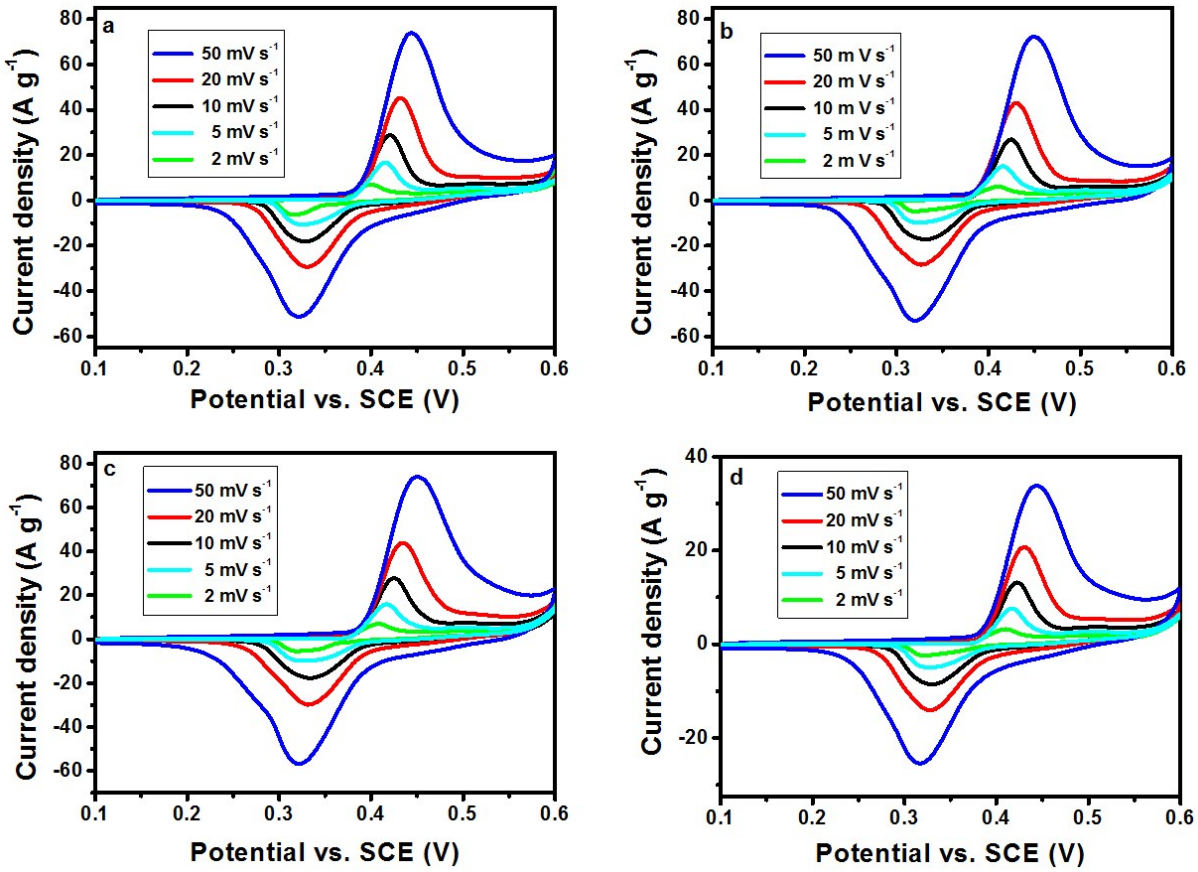

Fig. S4. CV curves of the as-prepared samples at various scan rates. (a) NONFs, (b) NOM-10, (c) NOM-30, and (d) NOM-40.

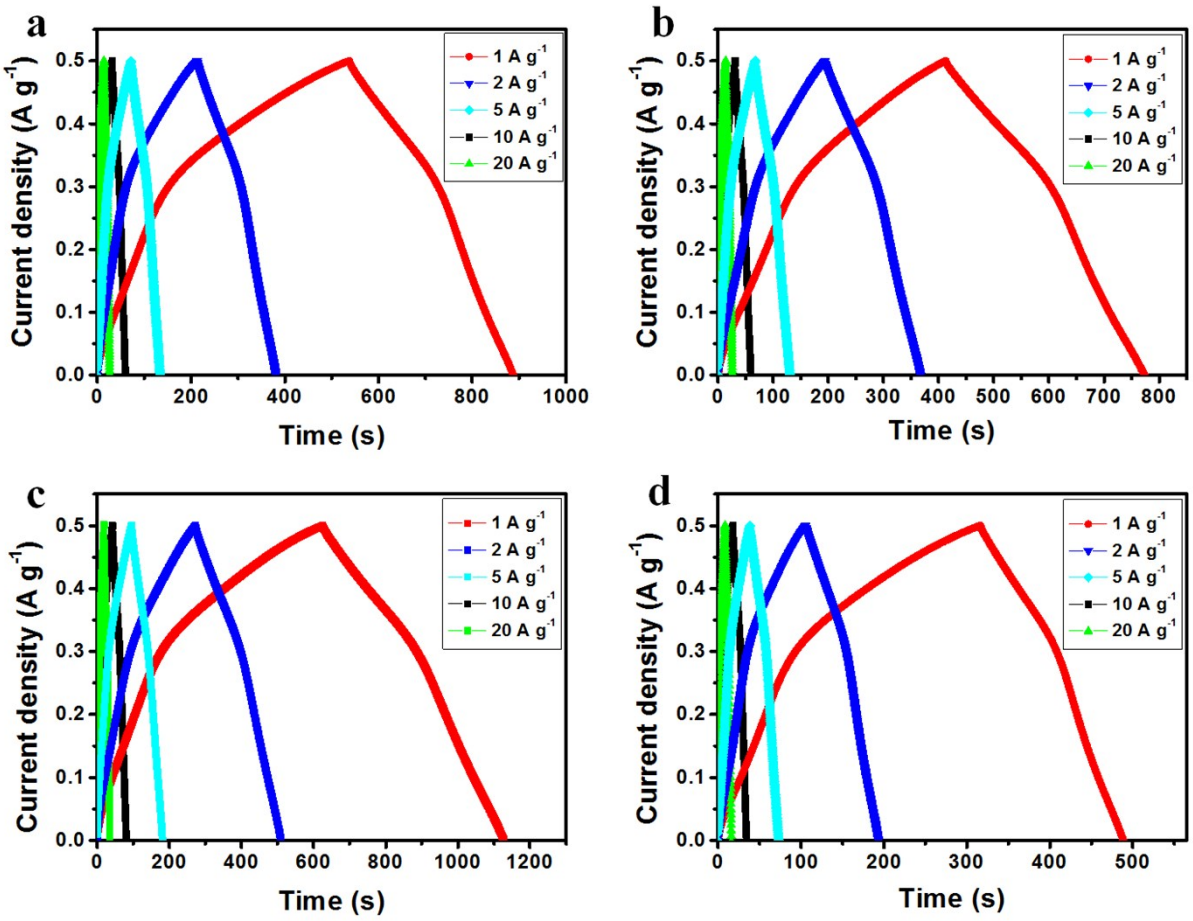

Fig. S5. GCD curves of the as-prepared samples at different current density ranging from 1.0 to 20 A g^{-1}. (a) NONFs, (b) NOM-10, (c) NOM-30, and (d) NOM-40.

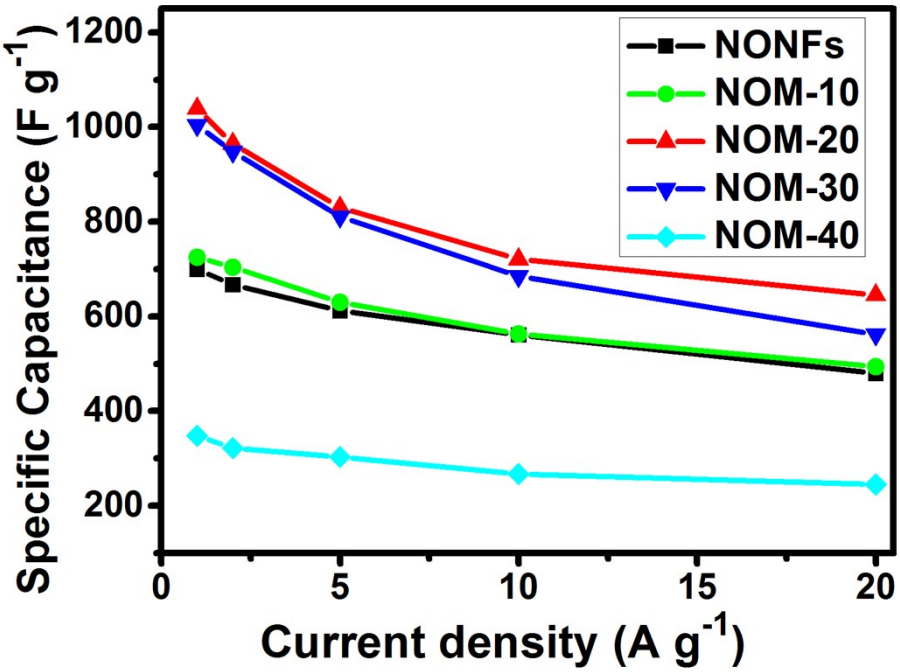

Fig. S6. Specific capacitance of the samples as a function of current density.

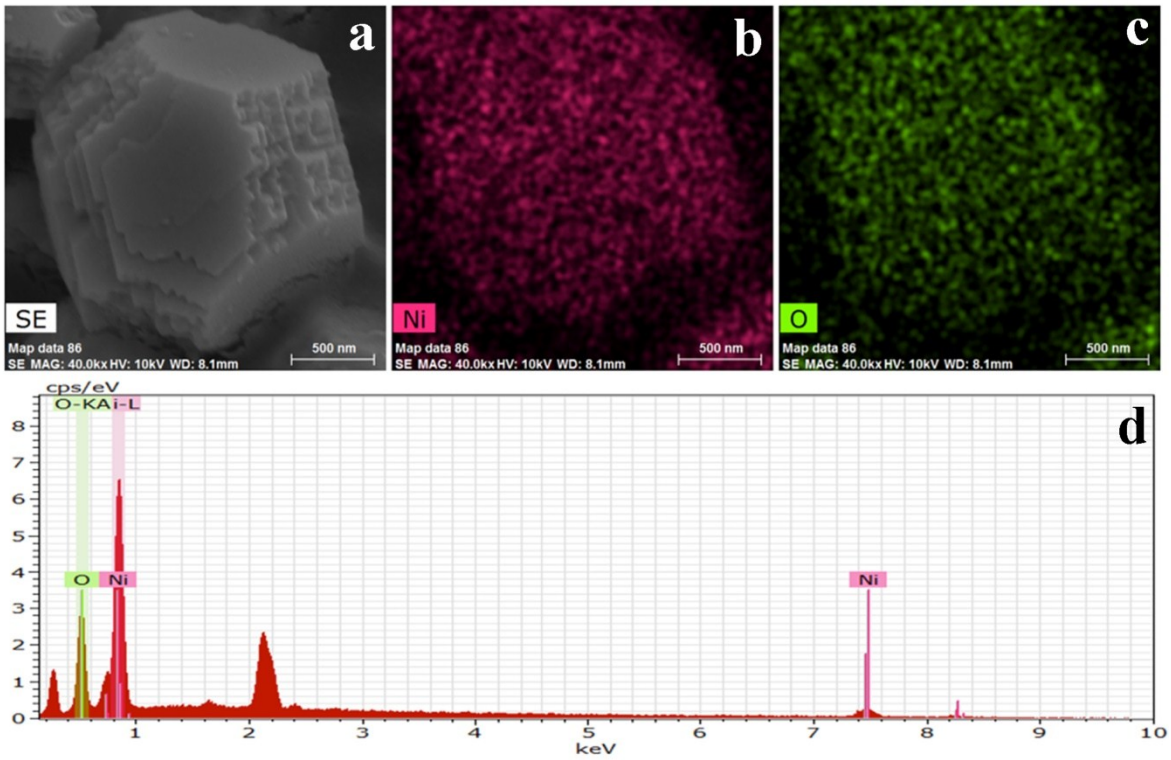

Fig. S7. FESEM image (a), corresponding element mapping images of Ni (b) and O (c), and EDS spectrum of the NOM-20 sample after 10,000 charge/discharge cycles.

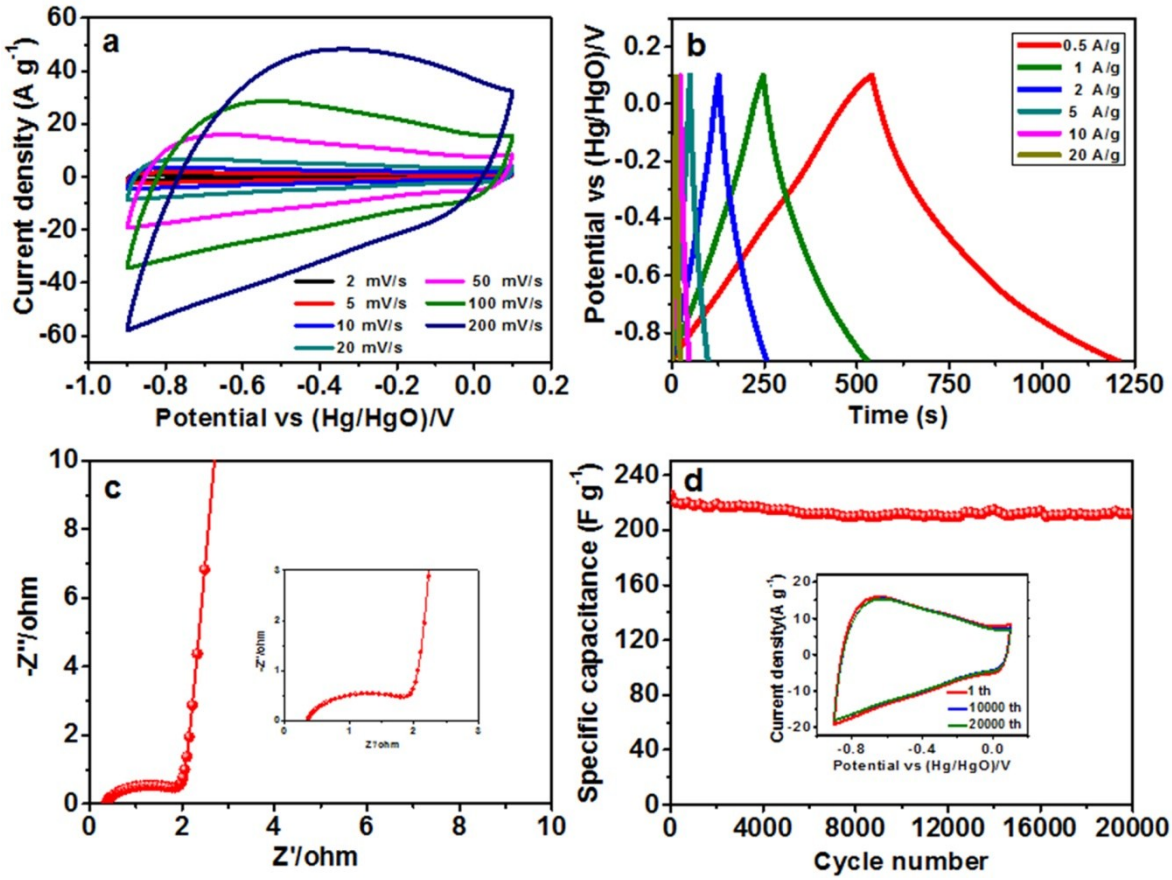

Fig. S8. Electrochemical performance of the employed 3DNG: (a) CV curves at various scan rates, (b) GCD curves at different current densities ranging from 0.5 to 20 A g^{-1}, (c) Electrochemical impedance spectroscopy (EIS) of 3DNG electrode, and (d) the cycling stability performance at constant current density of 10 A g^{-1}.

To explore the merits of 3DNG as negative electrode material for hybrid supercapacitors, the electrochemical performance for the employed 3DNG was tested in a three-electrode system with 2 M KOH aqueous solution as electrolyte. **Fig. S8a** depicts the CV curves of the employed 3DNG at different scan rates ranging from 2 to 200 mV s^{-1}. The specific capacitance calculated from the CV curves of 3DNG is ca. 274 F g^{-1} at a scan rate of 2 mV s^{-1}, and still retains ca.171 F g^{-1} even at an ultrahigh scan rate of 200 mV s^{-1}. **Fig. S8b** shows the GCD curves of the employed 3DNG at various current densities ranging from 0.5 to 20

A g^{-1}. The employed 3DNG exhibits an ultrahigh specific capacitance of ca. 334 F g^{-1} at a current density of 0.5 A g^{-1} from the slopes of the discharge curves. Especially, even at a very high current density of 20 A g^{-1}, the 3DNG still exhibits a high specific capacitance of ca. 225 F g^{-1}. **Fig. S8c** presents the characteristic impedance curve (Nyquist plots) for the 3DNG in the 2 M KOH electrolyte. The real axis intercept represents the combined resistance, including the ionic resistance of the electrolyte, electronic resistance of electrode materials, and contact resistance at the active material/current collector interface. As observed from the magnified image in the relatively high frequency region (Inset in **Fig. S8c**), the employed 3DNG shows a relatively low combined resistance of ca. 0.38 ohm, indicating a good electrical conductivity. The long-term cycling stability of the employed 3DNG was investigated using GCD at a high current density of 10 A g^{-1} (**Fig. S8d**). It can be clearly seen that the 3DNG presents an outstanding cycling stability and excellent capacitance retention of ca. 93% after 20 000 charge/discharge cycles. These results suggest that the as-employed 3DNG exhibits excellent electrochemical performance including high specific capacitance, good conductivity, remarkable stability, and outstanding reversibility when used as electrode material for supercapacitors.

Table S1. Comparison of the electrochemical performance for NiO micro/nanostructures.

Morphology	S_{BET} (m^2 g^{-1})	Specific capacitance (F g^{-1})	Electrolyte	Test conditions	Ref.
One-dimensional hierarchical hollow nanostructures	136.3	642	2.0 M KOH	3.0 A g^{-1}	S3
porous nanosheets	156	168	6.0 M KOH	1.0 A g^{-1}	S4
Spongy spheres	414	930	2.0 M KOH	15 A g^{-1}	S5
Porous thin film	--	839	1.0 M KOH	1 A g^{-1}	S6
Core-shell microspheres	196	448	5.0 M KOH	0.5 A g^{-1}	S7
Nanoflakes	107.5	137.7	2.0 M KOH	0.2 A g^{-1}	S8
Nanocolumns	102.4	390	1.0 M KOH	5 A g^{-1}	S9
Nanoflakes	--	401	2.0 M KOH	0.5 mA cm^{-2}	S10
Nanoflower	159	480	2.0 M KOH	0.5 A g^{-1}	S11
Hollow nanospheres	92.99	612.5	2.0 M KOH	0.5 A g^{-1}	S12
Porous hollow spheres	85	346	2.0 M KOH	1 A g^{-1}	S13
Hierarchical nanospheres	182	463	5.0 M KOH	4.5 A g^{-1}	S14
Hexagonal nanoplates	95	286.7	6.0 M KOH	1.0 A g^{-1}	S15
Hollow nanofibers	212.1	336	6.0 M KOH	5 mA cm^{-2}	S16
NiO/Ni nanocomposites	37	905	1.0 M KOH	1.0 A g^{-1}	S17
NiO/mesoporous carbons	802	880.2	6.0 M KOH	1.0 A g^{-1}	S18
Carbon-coated mesoporous NiO nanoparticles	107.6	931	1.0 M KOH	2.0 A g^{-1}	S19
Amorphous carbon-coated NiO nanofibers	144	288	1.0 M KOH	0.3 A g^{-1}	S20
NiO mesocrystals (NOM-20)	**197.5**	**1039**	**2.0 M KOH**	**1.0 A g^{-1}**	**This work**

References

(S1) Zhao, X.; Dong, H.; Xiao, Y.; Hu, H.; Cai, Y.; Liang, Y.; Sun, L.; Liu, Y.; Zheng, M. Three-Dimensional Nitrogen-Doped Graphene as Binder-Free Electrode Materials for Supercapacitors with High Volumetric Capacitance and the Synergistic Effect Between Nitrogen Configuration and Supercapacitive Performance. *Electrochim. Acta* **2016**, *218*, 32–40.

(S2) Singh, A. K.; Sarkar, D.; Khan, G. G.; Mandal, K. Unique Hydrogenated Ni/NiO coreshell 1D Nano-Heterostructures with Superior Electrochemical Performance as Supercapacitors. *J. Mater. Chem. A* **2013**, *1*, 12759–12767.

(S3) Zhang, G.; Yu, L.; Hoster, H. E.; Lou, X. W. Synthesis of One-Dimensional Hierarchical NiO Hollow Nanostructures with Enhanced Supercapacitive Performance. *Nanoscale* **2013**, *5*, 877–881.

(S4) Yuan, C. Template-Free Synthesis of Ultrathin Mesoporous NiO Nanosheets and Their Application in Supercapacitors. *Mater. Res. Bull*. **2013**, **48**, 840–843.

(S5) Liu, M.; Chang, J.; Sun, J.; Gao, L. Synthesis of Porous NiO Using $NaBH_4$ Dissolved in Ethylene Glycol as Precipitant for High-Performance Supercapacitor. *Electrochim. Acta* **2013**, *107*, 9–15.

(S6) Wang, H.; Wang, Y.; Wang, X. Pulsed Laser Deposition of the Porous Nickel Oxide Thin Film at Room Temperature for High-Rate Pseudocapacitive Energy Storage. *Electrochem. Commun.* **2012**, *18*, 92–95.

(S7) Han, D.; Xu, P.; Jing, X.; Wang, J.; Song, D.; Liu, J.; Zhang, M. Facile Approach to Prepare Hollow Core-shell NiO Microspherers for Supercapacitor Electrodes. *J. Solid State Chem.* **2013**, *203*, 60–67.

(S8) Zheng, Y. Z.; Ding, H. Y.; Zhang, M. L. Preparation and Electrochemical Properties of Nickel Oxide as a Supercapacitor Electrode Material. *Mater. Res. Bull.* **2009**, *44*, 403–407.

(S9) Zhang, X.; Shi, W.; Zhu, J.; Zhao, W.; Ma, J.; Mhaisalkar, S.; Maria, T. L.; Yang, Y.; Zhang, H.; Hng, H. H.; Yan, Q. Synthesis of Porous NiO Nanocrystals with Controllable Surface Area and Their

Application as Supercapacitor Electrodes. *Nano Res.* **2010**, *3*, 643–652.

(S10) Vijayakumar, S.; Nagamuthu, S.; Muralidharan, G. Supercapacitor Studies on NiO Nanoflakes Synthesized Through a Microwave Route. *ACS Appl. Mater. Interfaces* **2013**, *5*, 2188−2196.

(S11) Kim, S. I; Lee, J. S.; Ahn, H. J.; Song, H. K.; Jang, J. H. Facile Route to an Efficient NiO Supercapacitor with a Three-Dimensional Nanonetwork Morphology. *ACS Appl. Mater. Interfaces* **2013**, *5*, 1596−1603.

(12) Yang, Z.; Xu, F.; Zhang, W.; Mei, Z.; Pei, B.; Zhu, X. Controllable Preparation of Multishelled NiO Hollow Nanospheres via Layer-by-Layer Self-Assembly for Supercapacitor Application. J. *Power Sources* **2014**, *246*, 24–31.

(S13) Yan, X.; Tong, X.; Wang, J.; Gong, C.; Zhang, M.; Liang, L. Rational Synthesis of Hierarchically Porous NiO Hollow Spheres and Their Supercapacitor Application. Materials Letters 2013, 95, 1–4.

(S14) Han, D.; Xu, P.; Jing, X.; Wang, J.; Yang, P.; Shen, Q.; Liu, J.; Song, D.; Gao, Z.; Zhang, M. Trisodium Citrate Assisted Synthesis of Hierarchical NiO Nanospheres with Improved Supercapacitor Performance. *J. Power Sources* **2013**, *235*, 45–53.

(S15) Zhu, Z.; Ping, J.; Huang, X.; Hu, J.; Chen, Q.; Ji, X.; Banks, C. E. Hexagonal Nickel Oxide Nanoplate-Based Electrochemical Supercapacitor. *J. Mater. Sci.* **2012**, *47*, 503–507.

(S16) Ren, B.; Fan, M.; Liu, Q.; Wang, J.; Song, D.; Bai, X. Hollow NiO Nanofibers Modified by Citric Acid and the Performances as Supercapacitor Electrode. *Electrochim. Acta* **2013**, *92*, 197–204.

(S17) Lu, Q.; Lattanzi, M. W.; Chen, Y.; Kou, X.; Li, W.; Fan, X.; Unruh, K. M.; Chen, J. G.; Xiao, J. Q. Supercapacitor Electrodes with High-Energy and Power Densities Prepared from Monolithic NiO/Ni Nanocomposites. A*ngew. Chem. Int. Ed.* **2011**, *50*, 6847–6850.

(S18) Chen, F.; Zhou, W.; Yao, H.; Fan, P.; Yang, J.; Fei, Z.; Zhong, M. Self-Assembly of NiO Nanoparticles in Lignin-Derived Mesoporous Carbons for Supercapacitor Applications. *Green Chem.*

2013, *15*, 3057–3063.

(S19) Xu, K.; Zou, R.; Li, W.; Liu, Q.; Wang, T.; Yang, J.; Chen, Z.; Hu, J. Carbon-Coated Mesoporous NiO Nanoparticles as an Electrode Material for High Performance Electrochemical Capacitors. *New J. Chem.* **2013**, *37*, 4031–4036.

(S20) Shin, D. H.; Lee, J. S.; Jun, J.; Jang, J. Fabrication of Amorphous Carbon-Coated NiO Nanofibers for Electrochemical Capacitor Applications. *J. Mater. Chem. A* **2014**, *2*, 3364–3371.